J. Water Environ. Nanotechnol., 3(3): 254-264 Summer 2018

ORIGINAL RESEARCH PAPER

Enhanced Photocatalytic Performance of TiO_2 by β-Cyclodextrin for the Degradation of Organic Dyes

Asadollah Mohammadi [1,2]*, ***Seyed Hossein Mousavi*** [2]

[1] *Department of Chemistry, Faculty of Sciences, University of Guilan, Rasht, Iran*
[2] *Department of Water Engineering and Environment, Caspian Sea Basin Research Center, University of Guilan, Rasht, Iran*

Received: 2018.04.27 Accepted: 2018.06.08 Published: 2018.07.30

ABSTRACT

In this work, an efficient photocatalyst based on β-cyclodextrin-glycine-modified TiO_2 nanoparticles (TiO_2-Gly-βCD NPs) was successfully synthesized. The photocatalytic activity of the prepared TiO_2-Gly-βCD was tested on the degradation of methylene blue (MB) and methyl orange (MO) dyes. The enhanced surface properties of TiO_2-Gly-βCD photocatalyst generated excellent photocatalytic performance for the photocatalytic degradation of dyes in aqueous solution. These were strongly attributed to the presence of the functional hydroxyl groups and the inner cores of the hydrophobic cavity in β-CD to form inclusion complexes with organic molecules. As compared to the pure TiO_2 and TiO_2 modified by Gly, the dye degradation rate under UV irradiation was considerably enhanced by TiO_2/Gly/βCD as a photocatalyst. In addition, the sonocatalytic degradation of dyes was investigated, and it was found that the ultrasonic waves slightly enhanced the degradation time of dyes. The results indicated that the first-order kinetic model well describes the degradation of MB and MO dyes by TiO_2-Gly-βCD. Furthermore, the chemical oxygen demand (COD) values were determined for real industrial wastewater and treated wastewater.

Keywords: *Photocatalytic Degradation, Surface-Modification, TiO_2 Nanoparticles, TiO_2-Gly-βCD, Ultrasonic Degradation, β-Cyclodextrin*

How to cite this article
Mohammadi A, Mousavi SH. Enhanced Photocatalytic Performance of TiO_2 by β-Cyclodextrin for the Degradation of Organic Dyes. J. Water Environ. Nanotechnol., 2018; 3(3): 254-264. DOI: 10.22090/jwent.2018.03.006

INTRODUCTION

Cyclodextrins (CDs) are cyclic oligosaccharides with a hydrophobic inner cavity and characteristic truncated-cone shape that forms a well-defined cylindrical cavity. Due to the cylindrical cavity structure of CDs, they formed a kind of nonpolar microenvironment to allow a number of organic and inorganic pollutants to go in the inner cavity. Furthermore, CDs are environmentally friendly, water-soluble, and are commonly used in the food industry [1-6]. β-Cyclodextrin (β-CD) is one of the most common CDs, contains a hydrophobic cavity capable of forming inclusion complexes with many organic molecules. In addition, they are widely used as a dispersing reagent for insoluble chemicals and are commonly used for the chemical modification of nanomaterial surface to improve the adsorption and photocatalytic degradation activities toward metal ions and organic contaminants [7-12]. The coordinate bond between OH group of βCD and oxygen of TiO_2 results in adsorption of βCD on TiO_2 facilitating the photocatalytic activity of TiO_2 [13-16].

On the other hand, TiO_2 nanoparticles (TiO_2 NPs) have been investigated as a photocatalyst for various applications in wastewater treatment plants [17-20]. TiO_2 NPs showed many good features such as high activity, chemical stability, availability, non-toxicity, electronic and optical properties, high surface area, low cost and chemically stable

* Corresponding Author Email: *a_mohammadi@guilan.ac.ir*

and can be easily modified by chemical reactions to increase their photocatalytic and adsorption properties [21-25]. There are several ways to improve the photocatalytic activity of TiO_2 NPS: (i) control of particle size, crystallinity, and crystalline phases, (ii) doping with both organics (N, C, S) and cations, and (iii) surface modification with metals or semiconductors [26-31]. Despite these efforts, synthesis of efficient and commercially sufficient photocatalysts for important processes such as water splitting and degradation of various pollutants is still needed.

On the other hand, the rapid growth in the uses of organic contaminants in various industries and discharge without effective treatment in the processes of production and utilization has created serious health and safety problems for the environment and organisms [32-36]. In addition, most of the contaminants such as industrial aromatic dyes cannot be treated effectively by conventional methods such as physical adsorption. Industrial organic dyes are generally present in the colored wastewaters, which cannot be readily degraded, resulting in potential environmental problems [37-38]. In this work, a novel photocatalyst (TiO_2-Gly-βCD) was prepared and employed for the removal of some commercial organic dyes from aqueous solutions using the photocatalytic and ultrasonic degradation processes.

EXPERIMENTAL

Materials and Equipment

All the solvents and reagents were purchased from Sigma-Aldrich and Merck Chemical companies and used without any purification. Deionized water was purified with a Milli-Q water ion-exchange system and was used for the preparation of all solutions. The UV-visible absorption spectra were recorded by using a Pharmacia Biotech Spectrophotometer. Fourier transform infrared (FT-IR) spectra were recorded on a Shimadzu 8400 FT-IR spectrophotometer. The morphologies and phases of samples were investigated using a transmission electron microscopy (TEM, Zeiss - EM10C - 80 KV), field emission scanning electron microscope (FESEM, MIRA 3TESCAN-XMU), powder X-ray diffraction (XRD, Philips, PW 1800), and energy dispersive X-Ray (EDX, Hitachi Su 3500). The photocatalytic degradation of dyes was studied with a Nanoparticle UV-exciter (high-pressure mercury lamp, 500 W, 220 V). The ultrasonic irradiation was produced using an Ultrasonic (LABSONIC LBS2-4,5 model). The nitrogen adsorption-desorption isotherms were performed at -196 °C using a conventional volumetric apparatus (Bel Japan, BELSORP. Mini II). The specific surface area was calculated by Brunauer–Emmett–Teller (BET) method.

Preparation of TiO_2-Gly-βCD Photocatalyst

TiO_2 nanoparticles (TiO_2 NPs) were prepared by the sol-gel method using Titanium (IV) isopropoxide (TTIP) as a precursor according to previous reports [39]. In addition, the final product (TiO_2-Gly-βCD) as an efficient photocatalyst was synthesized according to our recently published article [40]. Scheme 1 shows the synthetic route of TiO_2-Gly-βCD catalyst.

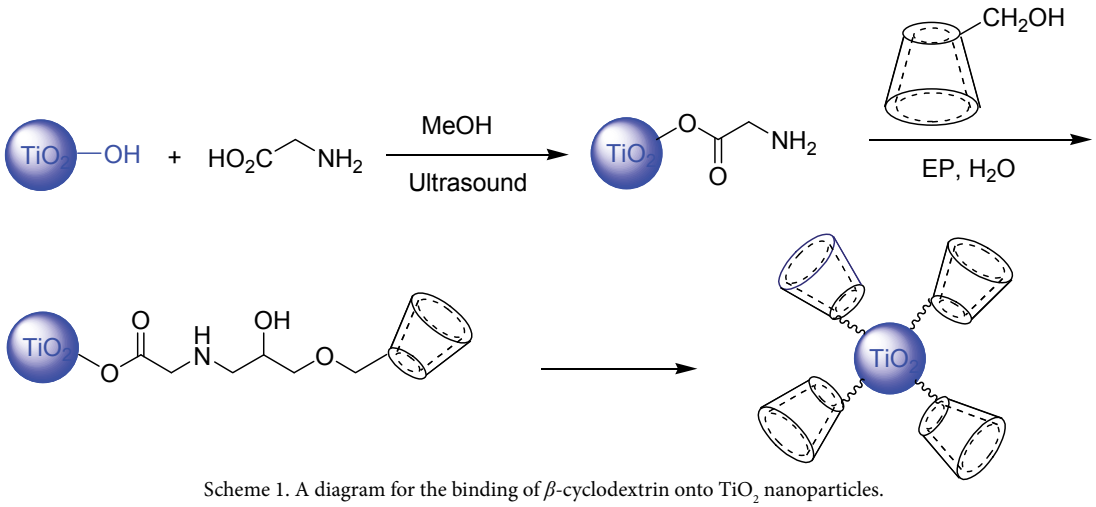

Scheme 1. A diagram for the binding of β-cyclodextrin onto TiO_2 nanoparticles.

Photo and Sonocatalytic Activity and Adsorption Tests

The photocatalytic activity of TiO_2-Gly-βCD was evaluated using the photodegradation of aqueous solutions of MB and MO dyes under UV light source. Fig. S1 (supporting information) shows the structure of the investigated dyes. A total of 0.1 g of TiO_2-Gly-βCD, as a photocatalyst, was added to 100 ml of aqueous dye solutions (30 mg/l) and then the suspension was stirred in the dark for 30 min in order to reach adsorption-desorption equilibrium. Then, the system was irradiated with a high-pressure mercury lamp (500 W, 220 V). At regular irradiation time intervals of 10 min, 10 ml sample was withdrawn and centrifuged to remove the catalyst and the concentration of MB and MO dyes was analyzed by UV-vis spectrophotometer. A similar test was conducted for sonocatalytic degradation of test dyes. The ultrasonic irradiation was produced by utilizing an ultrasonic bath of frequency 20 kHz (750 W). The maximum wavelength (λ_{max}) used for determination of the residual concentration of MB and MO dyes in supernatant solution was 660 nm, 460 nm, respectively. The concentration of the supernatant solution was obtained through the standard curve. The amount of dye adsorbed was determined by using the following equations:

$$q_e = \frac{(C_0 - C_e).V}{m} \quad (1)$$

$$\text{Removal}\ (\%) = \frac{100\ (C_0 - C_e)}{C_0} \quad (2)$$

where q_e (mg/g) is the adsorption capacity of adsorbent, C_0 and C_e (mg L^{-1}) are a concentration of the dye at the initial and equilibrium states, respectively, V (L) is the volume of the solution and m is the weight of adsorbent (g).

RESULTS AND DISCUSSION

Characterization of TiO_2-Gly-βCD Photocatalyst

Fig. 1 shows the FT-IR spectra of the pure TiO_2, TiO_2-Gly, and TiO_2-Gly-βCD NPs. In pure TiO_2, O-H stretching and bending vibrations in the FT-IR spectra were confirmed by the absorption bands at 3415 cm^{-1} and 1629 cm^{-1}, respectively. In addition, a broad absorption peak around 655 cm^{-1} is assigned to the Ti-O-Ti stretching band. In the case of the TiO_2 NPs modified by Gly, the high-intensity absorption peak at 1620 cm^{-1} is attributed to the carbonyl stretching band of Gly. The peaks at 3170 and 3423 cm^{-1} correspond to the NH stretching vibrations. These peaks show that glycine molecules have been bonded to the TiO_2 NPs. The FT-IR spectrum of TiO_2-Gly-βCD NPs showed the broad absorption band around 3388 cm^{-1}, which is related to the numerous hydroxyl and amino groups at the edge of the tubular structure of β-CD and the cross-linking bonds. The stretching vibration peak of the carbon-hydrogen bond (CH) in β-CD appears at 2924 cm^{-1}, and it demonstrates that the skeleton of β-CD is not been damaged. In addition, the absorption peaks at1032 and 1156 cm^{-1} are attributed to the antisymmetric glycosidic (C-O-C) vibrations and coupled (C-C/C-O) stretch vibration [41].

The FESEM pictures of the pure TiO_2, TiO_2-Gly, and TiO_2-Gly-βCD NPs are shown in Fig. 2(a-c). As can be seen from Fig. 2(a), the spherical

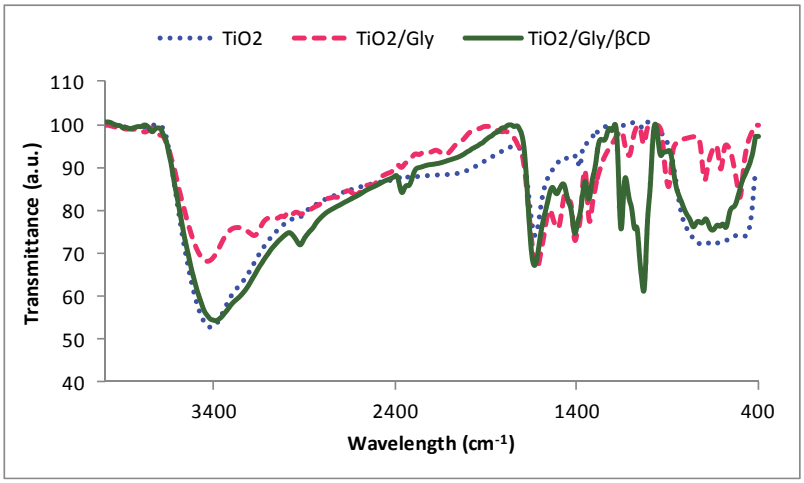

Fig. 1. FT-IR spectra of pure TiO_2, TiO_2-Gly, and TiO_2-Gly-βCD.

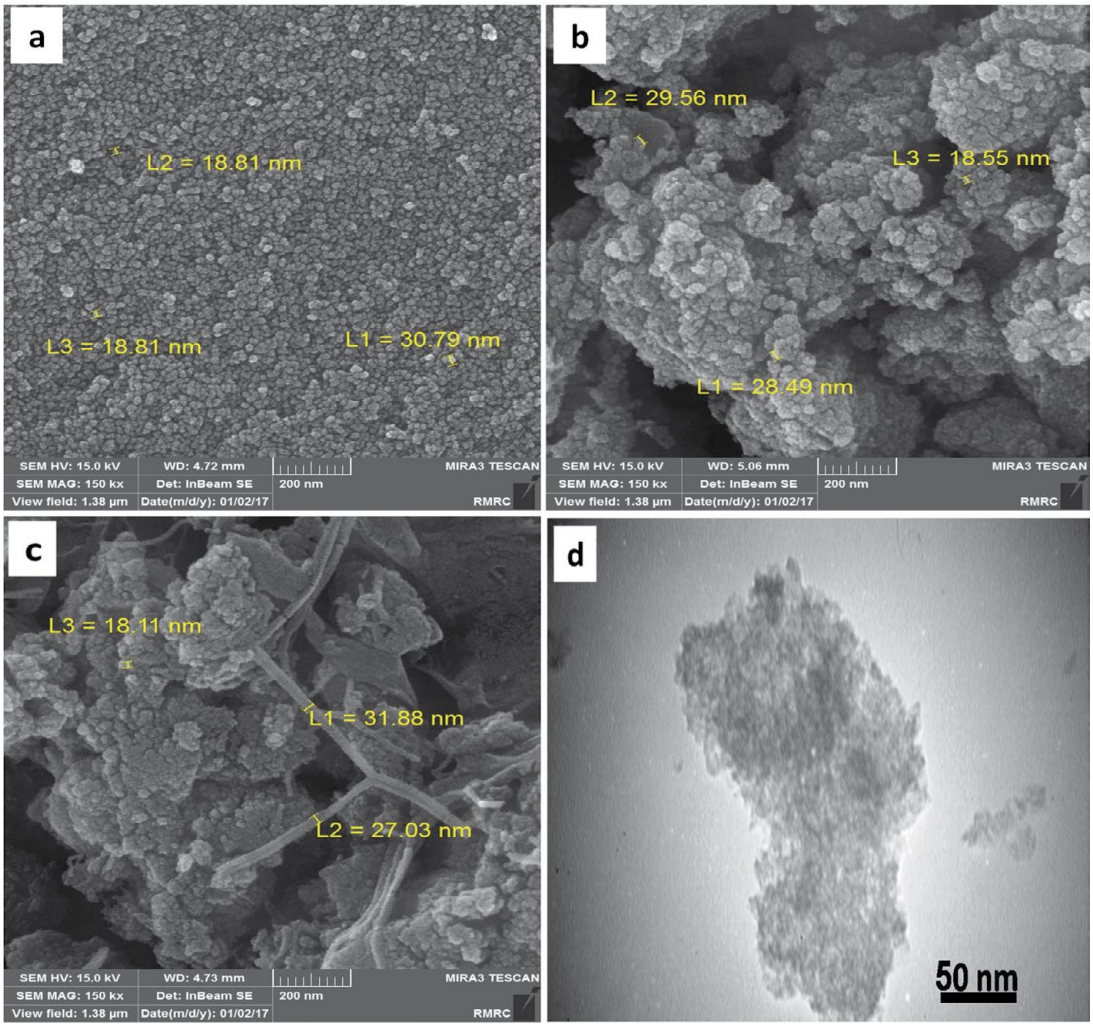

Fig. 2. FESEM images of samples. (a) TiO_2, (b) TiO_2-Gly, (c) TiO_2-Gly-βCD, and TEM image of the TiO_2-Gly-βCD (d).

morphology of TiO_2 NPs with nano dimensions is observed clearly. After the combination of the TiO_2 with the Gly under ultrasound conditions (Fig. 2(b)), and the surface modification using β-CD, the morphology of TiO_2 NPs surface was changed clearly. In the case of TiO_2-Gly-βCD, the spherical shape of TiO_2 NPs disappeared and some of the layers and nanorod-shaped materials were formed (Fig. 2(c)). In addition, the TEM images of the TiO_2-Gly-βCD with the size around 50 nm showed in Fig. 2(d). TEM images indicate the TiO_2-Gly-βCD was synthesized in nano-dimensions. These results showed that a large number of β-CDs have been attached to the surface of the nanoparticles, which can adsorb organic molecules from aqueous media.

Figs. S2-S4 (supporting information) show the XRD patterns, EDX and BET analyses for further characterization and confirmation of the product and intermediates. In addition, EDX elemental microanalysis of TiO_2, TiO_2-Gly, and TiO_2-Gly-βCD are listed in Table 1. The BET specific surface area, average pore diameter, and total pore volume of TiO_2-Gly-βCDs are 146.16 m^2/g, 10.73 nm, and 0.3923 cm^3/g, respectively. According to the obtained data, the prepared TiO_2-Gly-βCD can be classified as a mesopores material (type-IV isotherm) with a high BET surface area. The larger specific surface area of TiO_2-Gly-βCD is due to the presence of β-CD molecules on the adsorbent surface which has a large contact surface. In addition, the BET specific surface area of synthesized TiO_2-Gly-βCD is comparable to values from previously reported samples and the corresponding result is summarized in Table 2. Therefore, the results indicated that

Table 1. EDX elemental microanalysis (wt. %) of TiO_2, TiO_2-Gly, and TiO_2-Gly-βCD.

Sample	Normalized wt.%				
	Ti	O	C	N	Cl
TiO_2	46 %	49 %	5 %	-	-
TiO_2-Gly	35 %	40 %	20 %	5 %	-
TiO_2-Gly-βCD	38.5 %	44 %	15 %	2.25 %	0.25 %

Table 2. Specific surface area of TiO_2-Gly-βCD with other samples.

Sample	BET specific surface area (m^2/g)	Reference
TiO_2-Gly-βCD	146.16	This Work
TiO_2 (P25)	46.90	[42]
Titanate nanotubes (TNTs)	272.30	[42]
TiO_2-S	30.32	[43]
TiO_2-1.0C	67.22	[43]
Organic bentonite	32.74	[44]
Na-bentonite	74.35	[44]
GO-IPDI-CDs	32.13	[10]
$NiFe_2O_4$-NC	147.40	[45]

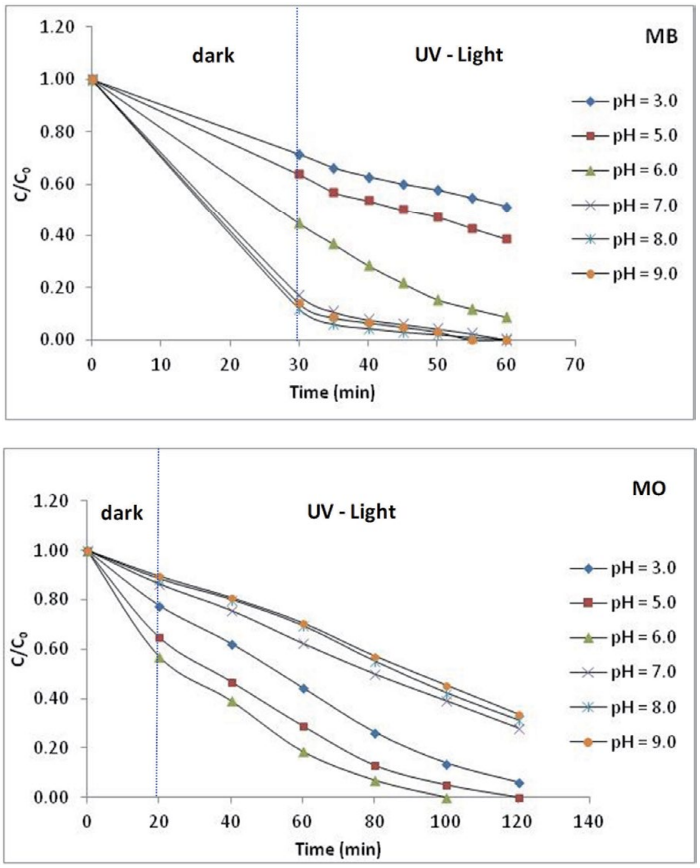

Fig. 3. Effect of pH on the photocatalytic degradation of dyes (C_0 = 30 ppm, catalyst dose = 0.01 g/l, T = 298 K).

the synthesized composite has a high specific surface area which can be used effectively for the treatment of wastewaters containing organic and inorganic contaminants.

Effect of pH on the Photocatalytic Degradation of Dyes

pH is one of the important factors in the removal of pollutants from water in the photocatalytic

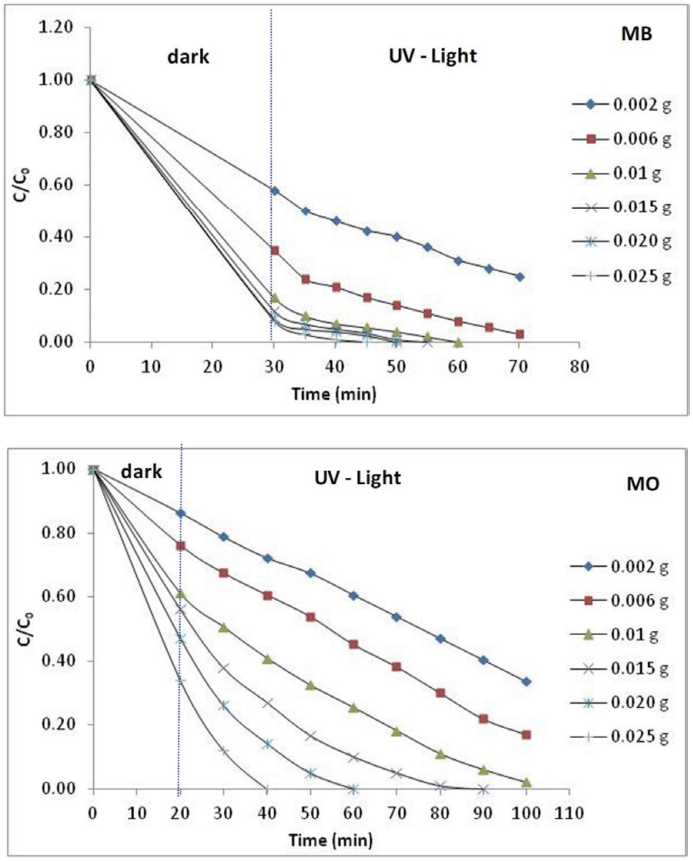

Fig. 4. Effect of catalyst dose on the photocatalytic degradation of dyes (C_0 = 30 ppm, Optimum pH values, T = 298 K).

degradation, adsorption, and other water treatment processes. The effects of pH on the photocatalytic degradation of investigated dyes were investigated over the range of 3.0 to 9.0, and the results are showed in Fig. 3. In the case of MB, the cationic dye, the degradation efficiency was increased with increasing pH value from 3.0 to 8.0 and then slowly decreased with the more increase of the pH from 8.0 to 9.0 for the photocatalytic process. In the case of MO, the anionic dye, the highest degradation was observed at the pH value of 6.0 and the degradation efficiency was decreased at the pH range from 7.0 to 9.0 as shown in Fig. 3. This might be due to the several amino and hydroxyl groups on the surface of TiO_2-Gly-βCD happened protonation at lower pH and then nano-particles can form hydrogen bonds with N atoms of MO structure. In the alkaline environment, the low removal efficiency is expected due to the repulsive forces between the TiO_2-Gly-βCD NPs and anionic MO dye. Additionally, in basic pH, hydroxyl ions (OH^-) in solution would compete with anionic dye molecules, which reduce the adsorption of anionic dye molecules [46]. According to the presence of hydroxyl and amino groups on the surface of the TiO_2-Gly-βCD, it can be used for various dyes in different pH condition of solutions. Meanwhile, these groups can produce electrostatic interactions with cationic MB dye in basic solution and electrostatic interactions with anionic MO dye in the acidic solution. Therefore, the optimum pH values for photocatalytic degradation of MB and MO dyes were 8.0 and 6.0, respectively. On the other hand, the removal of dyes on TiO_2-Gly-βCD continuously increased with time at optimum pH values. The rapid adsorption of organic dyes in the initial stages of the adsorption process can be attributed to the availability of numerous empty holes and a higher number of adsorption sites. Therefore, β-CD as a host-guest molecule entrapped dye molecules in its cavity and increased the interaction between TiO_2 and adsorbate molecules [42]. Furthermore, MB dye solution was discolored more rapidly by TiO_2-Gly-βCD (~100% discoloration after 30 min

UV irradiation) as compared with the MO (~100% discoloration after 80 min UV irradiation) in the optimum pH values.

Effect of Catalyst Amount on the Photocatalytic Degradation of Dyes

Catalyst dosage is an important quantitative variable in the water purification process using degradation method. The effect of the TiO_2-Gly-βCD dosage on the photodegradation of MB and MO dyes is shown in Fig. 4. The results showed that with the increase of catalyst amounts from 0.002 to 0.025 g, the degradation of dyes has increased continuously for the fixed solute concentration. It can be attributed to the accessibility of numerous empty holes and active sites of TiO_2-Gly-βCD catalyst. Most importantly, it is due to increased production of hydroxyl radicals ($^{\bullet}OH$). Furthermore, the results show that the degradation time of MB was 2.5 times was less than the degradation time for MO by TiO_2-Gly-βCD.

Effect of Initial Dye Concentration on the Photocatalytic Degradation of Dyes

The influence of initial dye concentration on the photocatalytic degradation of MB and MO dyes was studied. As can be seen from Fig. 5, after adsorption-desorption times, the degradation efficiency of investigated dyes was decreased with an increase in the dye concentration at optimum pH values. In other words, the generation of $^{\bullet}OH$ radicals by photocatalyst remain almost constant with an increase in the initial dye concentration of the solution, if the amount of catalyst was kept unchanged.

Comparison of the Photo and Sonocatalytic Activity of TiO_2-Gly-βCD

The sonocatalytic degradation of dyes was performed by TiO_2-Gly-βCD catalyst with an ultrasonic bath, operated with a fixed frequency of 59 kHz. Fig. 6 shows the sonocatalytic degradation of MB and MO dyes. The maximum degradation

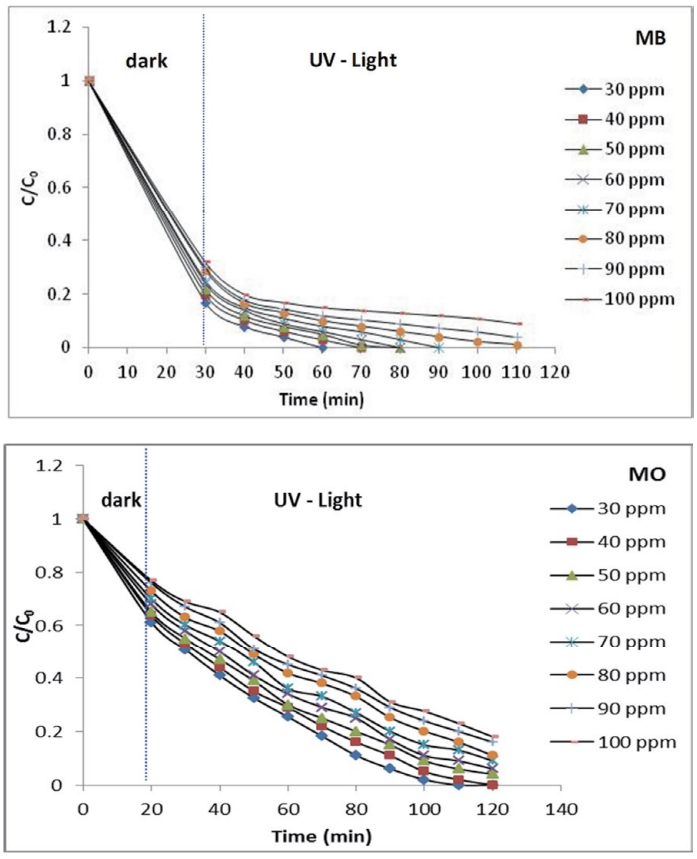

Fig. 5. Effect of initial dye concentration on the photocatalytic degradation of dyes (Optimum pH values, catalyst dose = 0.01 g/l, T = 298 K).

of MB and MO dyes (100 %) was observed in sonocatalytic system after 140 and 180 min of irradiation, respectively. As can be seen in Fig. 6, both MB and MO dyes were degraded completely in sonocatalytic system although it takes long times. It may be attributed to the enhanced mass transfer of dyes between the liquid phase and the TiO_2-Gly-βCD surface, as well as to the increased production of hydroxyl radicals in the solution. In addition, the degradation of investigated dyes in UV/TiO_2, UV/TiO_2-Gly, UV/TiO_2-Gly-βCD and US/TiO_2-Gly-βCD systems are compared in Fig. 7. The maximum decolorization of both MB and MO dyes was observed in UV/TiO_2-Gly-βCD system at the same irradiation times (80 min). These findings indicate that the degradation of dyes in UV/TiO_2-Gly-βCD system was much more effective than that with US/TiO_2-Gly-βCD system. In addition, decolorization efficiency was observed as 61% and 72% for MB and MO dyes in UV/TiO_2-Gly system, whereas in UV/TiO_2-Gly-βCD system 100% and 91% was observed, respectively. The increase in decolorization efficiency in UV/TiO_2-Gly-βCD system is attributed to the strong abilities of the multiple hydroxyl groups and the inner cores of the hydrophobic cavity in β-CD to adsorb investigated dyes. Additionally, the abilities of β-CD for inclusion-trapping of radicals generated by the TiO_2 are recognized. Furthermore, in comparison of MB, the degradation of MO dye in UV/TiO_2-Gly system was enhanced. It is indicated that the Glycine molecules on the surface of TiO_2-Gly can produce effective electrostatic interactions with anionic MO dye in the acidic solutions.

Photocatalytic Reaction Kinetic

The first-order kinetic model based on the Langmuir-Hinshelwood (L-H) model has been used to evaluate the photocatalytic reactions on the

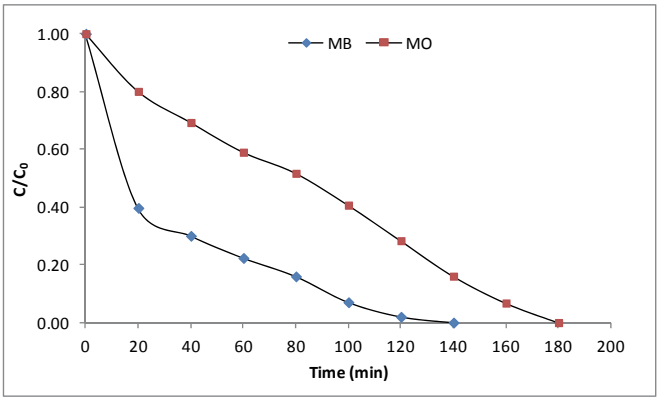

Fig. 6. Effect of contact time on the sonocatalytic degradation of dyes (C_0 = 30 ppm, Catalyst dose = 0.01 g/l, T = 298 K).

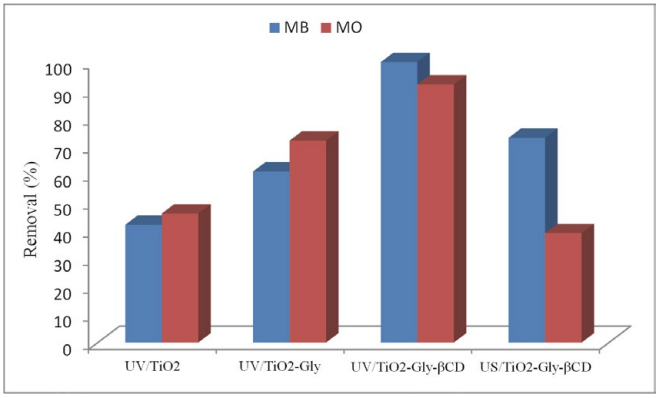

Fig. 7. Decolorization efficiency of dyes in UV/TiO_2, UV/TiO_2-Gly, UV/TiO_2-Gly-βCD and US/TiO_2-Gly-βCD systems (Contact time = 80 min., Optimum pH values, catalyst dose = 0.01 g/l, T = 298 K).

TiO_2/Gly/βCD NPs. The Langmuir-Hinshelwood model is expressed by the equation 1 [47-49].

$$\ln(C_o/C_t) = K_1 t \quad (3)$$

Where K_1 (min^{-1}) is the first-order rate constant for photocatalysis, C_o (mg/l) is the initial concentration of dye in aqueous solution at time t = 0; and C_t (mg/l) is the residual concentration of dye at time t (min). The linear relationship of $\ln(C_0/C_t)$ versus t (Fig. 8) has been drawn using the data in Fig. 3. Based on the first-order kinetic model, the correlation coefficients (R^2) values for the both MB and MO dyes are greater than 0.99. Therefore, the experimental kinetic data followed the first-order model in UV/TiO_2-Gly-βCD system. In addition, the rate constant (k) values using TiO_2-Gly-βCD under UV irradiation were observed to be 0.002 and 0.006 for MB and MO, respectively.

In addition, the possible reaction mechanism for the degradation of MB and MO dyes by using TiO_2-Gly-βCD as catalyst under UV irradiation has been expressed in Fig. 9.

Treatment of Textile Wastewater

In this study, we used TiO_2-Gly-βCD as an efficient photocatalyst for treatment of real textile wastewater (Iran Poplin Company). The chemical oxygen demand (COD) test was used for indirectly determination of the organic pollutants amount for treated wastewater and untreated wastewater. The investigated textile wastewater (pH = 8) was dark orange in color, which is due to the presence of reactive, acid blue 113, disperse dyes and other suspended materials. The treated wastewater (10 ml) was observed to be colorless and ~100% color was removed using synthesized photocatalyst (0.01 g, contact time = 15 min) at room temperature. In addition, the measured COD values for untreated wastewater and treated wastewater by TiO_2-Gly-βCD were 826 mg/l and 70 mg/L, respectively. This

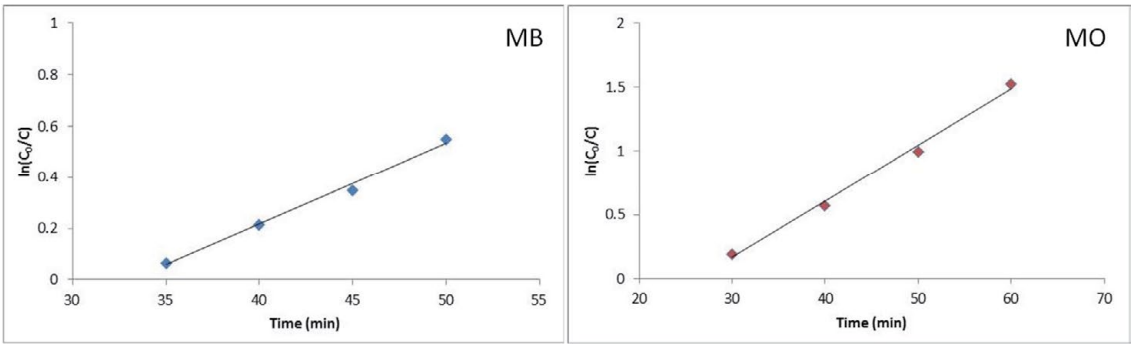

Fig. 8. Kinetics of photocatalytic degradation of MB and MO dyes using TiO_2-Gly-βCD.

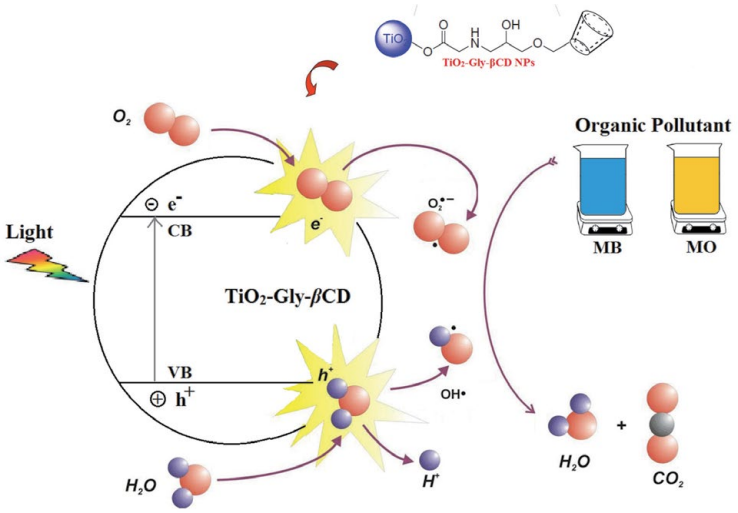

Fig. 9. Mechanism of photocatalytic degradation of dyes using TiO_2-Gly-βCD.

indicates that the calculated efficiency for treated wastewater based on COD test is 91% using TiO_2-Gly-βCD photocatalyst. Therefore, the results demonstrated that the synthesized photocatalyst has remarkable performance in removal of organic dyes and other contaminants from real textile wastewater.

CONCLUSION

TiO_2-Gly-βCD as an environmentally friendly catalyst was successfully synthesized and employed for the photocatalytic and ultrasonic degradation of some organic pollutants. The analysis results by FE-SEM, TEM, and BET show that the TiO_2-Gly-βCD nanocomposite was synthesized with particle size ranging from 20 to 45 nm. As compared to the pure TiO_2 and TiO_2 modified by Gly, the rate of degradation of MB and MO under UV irradiation was considerably enhanced using TiO_2-Gly-βCD as a catalyst. It was also noticed that the rate of degradation of dyes in UV/TiO_2-Gly-βCD system was much more effective as compared to US/TiO_2-Gly-βCD system. The dye degradation kinetic was also investigated using the first-order kinetic model. The results indicated that the first-order kinetic model well describes the degradation of MB and MO dyes using TiO_2-Gly-βCD as a catalyst.

ACKNOWLEDGMENTS

The authors are grateful to the Research Council of the University of Guilan for financial support of this research work.

SUPPLEMENTARY INFORMATION

Supplementary data to this article can be found online at http://www.jwent.net/

CONFLICTS OF INTEREST

The authors declare that there are no conflicts of interest.

REFERENCES

1. Guo Y, Guo S, Ren J, Zhai Y, Dong S, Wang E. Cyclodextrin Functionalized Graphene Nanosheets with High Supramolecular Recognition Capability: Synthesis and Host–Guest Inclusion for Enhanced Electrochemical Performance. ACS Nano. 2010;4(7):4001-10.
2. Rekharsky MV, Inoue Y. Complexation Thermodynamics of Cyclodextrins. Chemical Reviews. 1998;98(5):1875-918.
3. Saenger W, Jacob J, Gessler K, Steiner T, Hoffmann D, Sanbe H, et al. Structures of the Common Cyclodextrins and Their Larger AnaloguesBeyond the Doughnut. Chemical Reviews. 1998;98(5):1787-802.
4. Del Valle EMM. Cyclodextrins and their uses: a review. Process Biochemistry. 2004;39(9):1033-46.
5. Khan AR, Forgo P, Stine KJ, D'Souza VT. Methods for Selective Modifications of Cyclodextrins. Chemical Reviews. 1998;98(5):1977-96.
6. Atteia O, Del Campo Estrada E, Bertin H. Soil flushing: a review of the origin of efficiency variability. Reviews in Environmental Science and Bio/Technology. 2013;12(4):379-89.
7. Alarcón-Angeles G, Pérez-López B, Palomar-Pardave M, Ramírez-Silva MT, Alegret S, Merkoçi A. Enhanced host–guest electrochemical recognition of dopamine using cyclodextrin in the presence of carbon nanotubes. Carbon. 2008;46(6):898-906.
8. Wei M, Tian D, Liu S, Zheng X, Duan S, Zhou C. β-Cyclodextrin functionalized graphene material: A novel electrochemical sensor for simultaneous determination of 2-chlorophenol and 3-chlorophenol. Sensors and Actuators B: Chemical. 2014;195:452-8.
9. Fan L, Luo C, Sun M, Qiu H, Li X. Synthesis of magnetic β-cyclodextrin–chitosan/graphene oxide as nanoadsorbent and its application in dye adsorption and removal. Colloids and Surfaces B: Biointerfaces. 2013;103:601-7.
10. Yan J, Zhu Y, Qiu F, Zhao H, Yang D, Wang J, et al. Kinetic, isotherm and thermodynamic studies for removal of methyl orange using a novel β-cyclodextrin functionalized graphene oxide-isophorone diisocyanate composites. Chemical Engineering Research and Design. 2016;106:168-77.
11. Zhou Y, Sun L, Wang H, Liang W, Yang J, Wang L, et al. Investigation on the uptake and release ability of β-cyclodextrin functionalized Fe 3 O 4 magnetic nanoparticles by methylene blue. Materials Chemistry and Physics. 2016;170:83-9.
12. Zhao R, Wang Y, Li X, Sun B, Jiang Z, Wang C. Water-insoluble sericin/β-cyclodextrin/PVA composite electrospun nanofibers as effective adsorbents towards methylene blue. Colloids and Surfaces B: Biointerfaces. 2015;136:375-82.
13. Zhang X, Wu F, Wang Z, Guo Y, Deng N. Photocatalytic degradation of 4,4′-biphenol in TiO2 suspension in the presence of cyclodextrins: A trinity integrated mechanism. Journal of Molecular Catalysis A: Chemical. 2009;301(1-2):134-9.
14. Dimitrijevic NM, Rajh T, Saponjic ZV, de la Garza L, Tiede DM. Light-Induced Charge Separation and Redox Chemistry at the Surface of TiO2/Host–Guest Hybrid Nanoparticles. The Journal of Physical Chemistry B. 2004;108(26):9105-10.
15. Lu P, Wu F, Deng N. Enhancement of TiO2 photocatalytic redox ability by β-cyclodextrin in suspended solutions. Applied Catalysis B: Environmental. 2004;53(2):87-93.
16. Wang G, Wu F, Zhang X, Luo M, Deng N. Enhanced TiO2 photocatalytic degradation of bisphenol E by β-cyclodextrin in suspended solutions. Journal of Hazardous Materials. 2006;133(1-3):85-91.
17. Su W, Zhang Y, Li Z, Wu L, Wang X, Li J, et al. Multivalency Iodine Doped TiO2: Preparation, Characterization, Theoretical Studies, and Visible-Light Photocatalysis. Langmuir. 2008;24(7):3422-8.
18. Chatterjee D, Dasgupta S. Visible light induced photocatalytic degradation of organic pollutants. Journal of Photochemistry and Photobiology C: Photochemistry Reviews. 2005;6(2-3):186-205.
19. Fujishima A, Rao TN, Tryk DA. Titanium dioxide photocatalysis. Journal of Photochemistry and Photobiology

C: Photochemistry Reviews. 2000;1(1):1-21.
20. Ramaswamy V, Jagtap NB, Vijayanand S, Bhange DS, Awati PS. Photocatalytic decomposition of methylene blue on nanocrystalline titania prepared by different methods. Materials Research Bulletin. 2008;43(5):1145-52.
21. Mohamed RM, Ismail AA, Othman I, Ibrahim IA. Preparation of TiO2-ZSM-5 zeolite for photodegradation of EDTA. Journal of Molecular Catalysis A: Chemical. 2005;238(1-2):151-7.
22. Portela R, Canela MC, Sánchez B, Marques FC, Stumbo AM, Tessinari RF, et al. H2S photodegradation by TiO2/M-MCM-41 (M=Cr or Ce): Deactivation and by-product generation under UV-A and visible light. Applied Catalysis B: Environmental. 2008;84(3-4):643-50.
23. Belessi V, Lambropoulou D, Konstantinou I, Zboril R, Tucek J, Jancik D, et al. Structure and photocatalytic performance of magnetically separable titania photocatalysts for the degradation of propachlor. Applied Catalysis B: Environmental. 2009;87(3-4):181-9.
24. Bzdon S, Góralski J, Maniukiewicz W, Perkowski J, Rogowski J, Szadkowska-Nicze M. Radiation-induced synthesis of Fe-doped TiO2: Characterization and catalytic properties. Radiation Physics and Chemistry. 2012;81(3):322-30.
25. Wilson W, Manivannan A, Subramanian VR. Heterogeneous photocatalytic degradation of recalcitrant pollutants over CdS–TiO2 nanotubes: Boosting effect of TiO2 nanoparticles at nanotube–CdS interface. Applied Catalysis A: General. 2012;441-442:1-9.
26. Trevisan V, Olivo A, Pinna F, Signoretto M, Vindigni F, Cerrato G, et al. C-N/TiO2 photocatalysts: Effect of co-doping on the catalytic performance under visible light. Applied Catalysis B: Environmental. 2014;160-161:152-60.
27. Wang P, Zhou T, Wang R, Lim T-T. Carbon-sensitized and nitrogen-doped TiO2 for photocatalytic degradation of sulfanilamide under visible-light irradiation. Water Research. 2011;45(16):5015-26.
28. Kim M-S, Ryu CS, Kim B-W. Effect of ferric ion added on photodegradation of alachlor in the presence of TiO2 and UV radiation. Water Research. 2005;39(4):525-32.
29. Yang Y, Li X-j, Chen J-t, Wang L-y. Effect of doping mode on the photocatalytic activities of Mo/TiO2. Journal of Photochemistry and Photobiology A: Chemistry. 2004;163(3):517-22.
30. Binitha NN, Yaakob Z, Reshmi MR, Sugunan S, Ambili VK, Zetty AA. Preparation and characterization of nano silver-doped mesoporous titania photocatalysts for dye degradation. Catalysis Today. 2009;147:S76-S80.
31. Mohammadi A, Aliakbarzadeh Karimi A. Methylene Blue Removal Using Surface-Modified TiO2 Nanoparticles: A Comparative Study on Adsorption and Photocatalytic Degradation. Journal of Water and Environmental Nanotechnology. 2017; 2:118-128.
32. Sun H, Zhao X, Zhang L, Fan W. Origin of the Enhanced Visible Photocatalytic Activity in (N, C)-Codoped ZnS Studied from Density Functional Theory. The Journal of Physical Chemistry C. 2011;115(5):2218-27.
33. Kyung H, Lee J, Choi W. Simultaneous and Synergistic Conversion of Dyes and Heavy Metal Ions in Aqueous TiO2Suspensions under Visible-Light Illumination. Environmental Science & Technology. 2005;39(7):2376-82.
34. Saeed A, Sharif M, Iqbal M. Application potential of grapefruit peel as dye sorbent: Kinetics, equilibrium and mechanism of crystal violet adsorption. Journal of Hazardous Materials. 2010;179(1-3):564-72.
35. Liu L, Liu Z, Bai H, Sun DD. Concurrent filtration and solar photocatalytic disinfection/degradation using high-performance Ag/TiO2 nanofiber membrane. Water Research. 2012;46(4):1101-12.
36. Ochiai T, Fujishima A. Photoelectrochemical properties of TiO2 photocatalyst and its applications for environmental purification. Journal of Photochemistry and Photobiology C: Photochemistry Reviews. 2012;13(4):247-62.
37. Kadirvelu K, Karthika C, Vennilamani N, Pattabhi S. Activated carbon from industrial solid waste as an adsorbent for the removal of Rhodamine-B from aqueous solution: Kinetic and equilibrium studies. Chemosphere. 2005;60(8):1009-17.
38. Chatzisymeon E, Xekoukoulotakis NP, Coz A, Kalogerakis N, Mantzavinos D. Electrochemical treatment of textile dyes and dyehouse effluents. Journal of Hazardous Materials. 2006;137(2):998-1007.
39. Moafi HF, Shojaie AF, Zanjanchi MA. Titania and titania nanocomposites on cellulosic fibers: Synthesis, characterization and comparative study of photocatalytic activity. Chemical Engineering Journal. 2011;166(1):413-9.
40. Mousavi SH, Mohammadi A. A cyclodextrin/glycine-functionalized TiO 2 nanoadsorbent: Synthesis, characterization and application for the removal of organic pollutants from water and real textile wastewater. Process Safety and Environmental Protection. 2018;114:1-15.
41. Cannavà C, Crupi V, Ficarra P, Guardo M, Majolino D, Stancanelli R, et al. Physicochemical characterization of coumestrol/β-cyclodextrins inclusion complexes by UV–vis and FTIR-ATR spectroscopies. Vibrational Spectroscopy. 2008;48(2):172-8.
42. Liu W, Ni J, Yin X. Synergy of photocatalysis and adsorption for simultaneous removal of Cr(VI) and Cr(III) with TiO2 and titanate nanotubes. Water Research. 2014;53:12-25.
43. Simonetti EAN, de Simone Cividanes L, Campos TMB, de Menezes BRC, Brito FS, Thim GP. Carbon and TiO 2 synergistic effect on methylene blue adsorption. Materials Chemistry and Physics. 2016;177:330-8.
44. Huang Z, Li Y, Chen W, Shi J, Zhang N, Wang X, et al. Modified bentonite adsorption of organic pollutants of dye wastewater. Materials Chemistry and Physics. 2017;202:266-76.
45. Naushad M, Ahamad T, Al-Maswari BM, Abdullah Alqadami A, Alshehri SM. Nickel ferrite bearing nitrogen-doped mesoporous carbon as efficient adsorbent for the removal of highly toxic metal ion from aqueous medium. Chemical Engineering Journal. 2017;330:1351-60.
46. Crini G, Peindy H, Gimbert F, Robert C. Removal of C.I. Basic Green 4 (Malachite Green) from aqueous solutions by adsorption using cyclodextrin-based adsorbent: Kinetic and equilibrium studies. Separation and Purification Technology. 2007;53(1):97-110.
47. Fu M, Li Y, wu S, Lu P, Liu J, Dong F. Sol–gel preparation and enhanced photocatalytic performance of Cu-doped ZnO nanoparticles. Applied Surface Science. 2011;258(4):1587-91.
48. Sun J-h, Wang Y-k, Sun R-x, Dong S-y. Photodegradation of azo dye Congo Red from aqueous solution by the WO3–TiO2/activated carbon (AC) photocatalyst under the UV irradiation. Materials Chemistry and Physics. 2009;115(1):303-8.
49. Trandafilović LV, Jovanović DJ, Zhang X, Ptasińska S, Dramićanin MD. Enhanced photocatalytic degradation of methylene blue and methyl orange by ZnO:Eu nanoparticles. Applied Catalysis B: Environmental. 2017;203:740-52.